Published in final edited form as:
Ann Surg Oncol. 2007 February ; 14(2): 286–298.

Lymphatic Drainage of the Peritoneal Space: A Pattern Dependent on Bowel Lymphatics

Cherie P. Parungo, M.D.[*], **David I. Soybel, M.D.**[*], **Yolonda L. Colson, M.D., Ph.D.**[*], **Sang-Wook Kim, Ph.D.**[†], **Shunsuke Ohnishi, M.D., Ph.D.**[‡], **Alec M. De Grand, M.B.A.**[‡], **Rita G. Laurence, B.S.**[*], **Edward G. Soltesz, M.D.**[*], **Fredrick Y. Chen, M.D.**[*], **Lawrence H. Cohn, M.D.**[*], **Moungi G. Bawendi, Ph.D.**[†], and **John V. Frangioni, M.D., Ph.D.**[‡]

[*]*Department of Surgery, Brigham & Women's Hospital, Boston, MA*

[†]*Department of Chemistry, Massachusetts Institute of Technology, Cambridge, MA*

[‡]*Division of Hematology/Oncology and Department of Radiology, Beth Israel Deaconess Medical Center, Boston, MA*

Abstract

Background—Understanding lymph drainage patterns of the peritoneum could assist in staging and treatment of gastrointestinal and ovarian malignancies. Sentinel lymph nodes (SLNs) have been identified for solid organs and the pleural space. Our purpose was to determine whether the peritoneal space had a predictable lymph node drainage pattern.

Methods—Rats received intraperitoneal injection of near-infrared (NIR) fluorescent tracers, namely quantum dots (QDs; designed for retention in SLNs) or HSA800 (designed for lymphatic flow beyond the SLN). A custom imaging system detected NIR fluorescence at 10 and 20 minutes and 1, 4, and 24 hours after injection. To determine the contribution of viscera on peritoneal lymphatic flow, additional cohorts received bowel resection prior to NIR tracer injection. Associations with appropriate controls were assessed with the chi square test.

Results—QDs drained to celiac, superior mesenteric, and periportal lymph node groups. HSA800 drained to these same groups at early time points, but continued flowing to mediastinal lymph nodes via the thoracic duct. After bowel resection, both tracers were found in thoracic, not abdominal, lymph node groups. Additionally, HSA800 was no longer found in the thoracic duct but in the anterior chest wall and diaphragmatic lymphatics.

Conclusions—The peritoneal space drains to celiac, superior mesenteric, and periportal lymph node groups first. Lymph continues via the thoracic duct to mediastinal lymph nodes. Bowel lymphatics are a key determinant of peritoneal lymph flow, as bowel resection shifts lymph flow directly to intrathoracic lymph nodes via chest wall lymphatics.

Keywords

Peritoneal Space; Lymph Node; Lymphatic Drainage; Near-infrared Fluorescence; Carcinomatosis; Metastasis

Corresponding Author: John V. Frangioni, M.D., Ph.D., Division of Hematology/Oncology, Beth Israel Deaconess Medical Center, 330 Brookline Avenue, Room SL-B05, Boston, MA, 02215, Phone: (617) 667-0692 Fax: (617) 667-0981, Email: jfrangio@bidmc.harvard.edu.

SYNOPSIS

Lymphatic drainage from the peritoneum proceeds in parallel fashion to multiple yet specific intraabdominal sentinel lymph node groups. Lymph flow continues to intrathoracic lymph nodes primarily via the thoracic duct. Resection of visceral lymphatics diverts peritoneal lymph flow to intrathoracic lymph nodes via diaphragmatic and anterior chest wall lymphatics.

INTRODUCTION

The sentinel lymph node (SLN) concept states that the first lymph node to receive lymphatic drainage from a tumor site will contain tumor cells in the setting of direct lymphatic spread.[1] Sentinel lymph node mapping has had increasing applications in solid organs and masses. Two recent studies demonstrated that a potential space, the pleural space, also drains via a SLN. Novel near-infrared (NIR) fluorescent lymph tracers identified the superior mediastinal lymph node group as the SLN of the pleural space,[2] and patterned drainage of lymph to chest wall, axillary, and intraabdominal lymph node groups followed.[3]

However, it remains controversial whether the peritoneal space has a predictable lymph drainage pattern. Studies utilizing injection of Evans blue dye or radioactively labeled albumin into the peritoneal cavity have demonstrated lymph drainage to both mediastinal and intraabdominal lymph nodes.[4] However, abdominal lymph nodes were difficult to characterize against a high background of blue color or radioactivity within the abdomen. These earlier studies described lymph transport through channels in the diaphragm,[5] lymphatic duct,[6] or a remnant pneumoenteric fistula.[7] Although these previous studies have identified lymph channels communicating with the peritoneal space, none has mapped predictable drainage patterns or SLN groups.

Elucidation of the patterns of lymphatic drainage of the peritoneal space could assist in staging, prognosis, and treatment of intraabdominal malignancies with potential for tumor sloughing into the peritoneal space. If predictable SLNs of the peritoneal space could be identified, they could be investigated or biopsied for tumor involvement even before bulky lymph node involvement was clinically apparent. The purpose of this study was to investigate the lymphatic drainage of the peritoneal space by answering three questions: Does the peritoneum have a SLN? What is the pattern of lymph flow beyond the SLN? Which peritoneal surface, visceral or parietal, governs intraperitoneal lymphatic flow?

To address these questions, we employed two novel NIR fluorescent lymph tracers: quantum dots (QDs) and human serum albumin (HSA) conjugated with IRDye800 (HSA800). QDs have a hydrodynamic diameter of 20 nm and are engineered to travel through lymph channels but stop within the first encountered lymph node. In contrast, HSA800 has a hydrodynamic diameter of 7 nm, which allows travel through lymphatics and lymph nodes to identify distant patterns of lymph flow. With QDs identifying SLNs, and HSA800 identifying distant lymph flow, we were able to characterize lymphatic flow from the peritoneal space.

MATERIALS AND METHODS

Preparation of QDs for Identification of SLNs

NIR fluorescent quantum dots (QDs) designed for retention in the first draining lymph node have been previously described.[8] Briefly, these type-II core/shell QDs are semiconductor nanocrystals that contain an inorganic core of cadmium telluride, an inorganic shell of cadmium selenide, and an outer organic coating of solubilizing oligomeric phosphines. Hydrodynamic diameter measured by gel filtration is 15–20 nm. These particular QDs were engineered to

fluoresce in the NIR, with peak emission at 840 nm. A stock solution of 0.2 mM QDs in phosphate buffered saline (PBS), pH 7.4 was used for all studies.

Preparation of HSA800 for Identification of Distant Lymph Flow

HSA800, designed with a hydrodynamic diameter of 7 nm for migration to distant lymph nodes after initial accumulation in the first draining node, has been described in detail previously.[9] Briefly, human serum albumin (HSA) was covalently conjugated to IRDye™ 800CW NIR dye (CW800; LI-COR, Lincoln, NE) via an amide bond (HSA800). The ratio of CW800 to albumin was 3.4. Peak absorbance and emission of HSA800 were 778 nm and 795 nm, respectively, in phosphate buffered saline, pH 7.4. A stock solution of 10 μM HSA800 in PBS was used for all studies. Both of these fluorescent biologic labels are excellent tracers for SLN mapping since they are highly fluorescent, nonradioactive, and easily visible deep within tissue.

Intraoperative NIR Fluorescence Imaging System

The imaging system has been described in detail previously.[10] Briefly, it is composed of two wavelength-isolated excitation sources, one generating 400–700 nm "white" light, and the other simultaneously generating 5 mW/cm^2 of 725–775 nm light over a 15 cm diameter field of view. Photon collection is achieved with custom-designed optics that maintain separation of the white light and NIR fluorescence (> 795 nm) channels. After computer-controlled camera acquisition, anatomic (white light) and functional (NIR fluorescent light) images can be displayed separately and merged. To create a single image that displays both anatomy (color video) and function (NIR fluorescence), the NIR fluorescence image was pseudo-colored in lime green and overlaid with 100% transparency on top of the color video image of the same surgical field. All images are refreshed 15 times per second. The entire apparatus is suspended on an articulated arm over the surgical field, thus permitting noninvasive and nonintrusive imaging. Real-time video images assisted in the location and dissection of HSA800-positive tissue. Depending on the application, fluorescence can be detected through up to 1 cm of tissue.[8]

Animal Surgery

Animals were used under the supervision of an approved institutional protocol. Adult male Sprague-Dawley rats (Taconic, Germantown, NY) of 250 g were anesthetized with xylazine (10 mg/kg) and ketamine (100 mg/kg) intraperitoneally. Rats were shaved, prepped, and draped in the usual sterile fashion.

Protocol 1: To identify whether the peritoneal space has dominant SLN drainage—Under aseptic conditions, a 0.5 cm midline laparotomy was made. The abdominal wall was elevated away from the abdominal contents to ensure tracer injection into the peritoneal space and to avoid injection into tissue. QDs (5.7 μM, 300 μL/animal, 1.7 nmol/animal, 6.8 nmol/kg body weight) were administered into 20 rats using a 25-gauge needle. QDs, with a large hydrodynamic diameter 20 nm, were chosen as a tracer of the SLN because of their ability to flow through lymphatics, but remain in the first draining lymph node, i.e., the SLN. During administration of QDs, NIR fluorescence imaging of the peritoneum was used to demonstrate even distribution of the QDs throughout the peritoneal space. The laparotomy was sutured closed followed by closure of the skin. Four rats were imaged at the time points of 10 minutes, 20 minutes, 1, 4, and 24 hours to visualize lymph nodes containing QDs.

Protocol 2: To determine whether the location of QD injection alters the pattern of SLN drainage of the peritoneum—Under aseptic conditions, a 0.5 cm incision in the right upper, right lower, left upper, or left lower abdominal wall was made. The abdominal wall was elevated away from the abdominal contents to ensure NIR tracer injection into the

peritoneal space and to avoid injection into tissue. QDs (5.7 μM, 300 μL/animal, 1.7 nmol/animal, 6.8 nmol/kg body weight) were administered into one of the four quadrants of the abdomen (n = 4 rats for each quadrant) using a 25-gauge needle. Rats were imaged at 1 hour.

Protocol 3: To identify peritoneal lymph node drainage patterns beyond the SLN—A 0.5 cm midline laparotomy was made. The abdominal wall was elevated away from the abdominal contents to ensure NIR tracer injection into the peritoneal space and to avoid injection into tissue. HSA800 (10 μM, 300 μL/animal, 3 nmol/animal, 12 nmol/kg) was injected into the peritoneal space of 20 rats using a 25-gauge needle. The small laparotomy was sutured closed followed by closure of the skin. HSA800 was chosen as a tracer of lymph patterns beyond the SLN because of its small diameter of 7 nm, which permits flow through lymph nodes. Four rats were imaged at the time points of 10 minutes, 20 minutes, 1 hour, and 24 hours to identify HSA800 within lymphatics and lymph nodes.

Protocol 4: To identify whether the location of HSA injection alters the identified drainage pattern of peritoneal flow—HSA800 (dye concentration 10 μM, 300 μL/animal, 3 nmol/animal, 12 nmol/kg) was injected into each of the four quadrants of the abdomen through a laparotomy in the right upper, right lower, left upper, or left lower quadrant (n = 4 rats for each quadrant). Rats were imaged at 1 hour.

Protocol 5: To measure the contribution of visceral surfaces on peritoneal lymph flow of QDs—Twelve rats underwent resection of bowel from the ligament of Treitz to the sigmoid colon and anastomosis of the duodenum to the sigmoid colon with six interrupted sutures of 6-0 silk. This resection was the maximal resection possible while still maintaining continuity and preservation of the celiac, superior mesenteric, and periportal lymph node groups. Six of these rats received intraperitoneal injection of QDs. Six rats underwent a sham operation consisting of a laparotomy bowel transection at the ligament of Treitz and reanastomosis without resection using six interrupted sutures of 6-0 silk. All 12 rats underwent midline injection of QDs (5.7 μM, 300 μL/animal, 1.7 nmol/animal, 6.8 nmol/kg body weight) with imaging of SLNs 1 hour after injection.

Protocol 6: To measure the contribution of visceral surfaces on peritoneal lymph flow of HSA800—Six rats underwent resection of bowel as described in Protocol 5. Six additional control rats underwent laparotomy, bowel transection, and anastomosis. All 12 rats received intraperitoneal injection of HSA800 (10 μM, 300 μL/animal, 3 nmol/animal, 12 nmol/kg). All animals were imaged 1 hour after injection.

Statistical Analysis

Associations were assessed with the chi square test with distributions considered significant if $p < 0.05$.

RESULTS

Identification of Peritoneal SLNs Using Large Hydrodynamic Diameter QDs

Ten minutes after injection of QDs into the peritoneal space, QDs were still apparent throughout the peritoneum. In one of the four rats, the superior mesenteric lymph node had QD uptake. Twenty minutes after injection of QDs, minimal QDs remained in the peritoneum. One to three intraabdominal lymph node groups demonstrated QD uptake at this time point in all animals. The QD-positive lymph node groups included the superior mesenteric (Figure 1A), celiac, and periportal lymph node groups. At time points of 1, 4, and 24 hours this pattern was not significantly different (Figure 1B). Minimal QD uptake was observed in the superior mediastinal lymph node group, but the brightness of this uptake was far inferior to those lymph

nodes of the abdomen noted above. The superior mesenteric, celiac, and periportal lymph node groups were the dominant recipients of lymphatic uptake from the peritoneal space.

Identification of Peritoneal Lymph Drainage beyond the SLN Using Small Hydrodynamic Diameter HSA800

Ten minutes after injection of HSA800 into the peritoneal space, HSA800 was still apparent throughout the peritoneal space, but in two rats HSA800 was found in two superior mesenteric lymph nodes. By 20 minutes, no HSA800 was visible within the peritoneum. All four rats had uptake of HSA800 into the superior mesenteric and celiac lymph nodes. Three of the four had uptake into the periportal lymph node group and one had uptake of HSA800 into the superior mediastinal lymph node group. At 1, 4, and 24 hours, rats had consistent uptake into the superior mesenteric, celiac, periportal, and superior mediastinal lymph node groups and occasional uptake into the anterior mediastinal lymph node groups (Figure 2A). There were specific positive and negative lymph node groups suggesting a distinct lymph node pattern, not a diffuse distribution of HSA800 to all lymph tissues (Figure 2B). There was no significant difference in the location or number of node groups with HSA800 uptake between 1, 4, and 24 hours. In contrast to QDs, which remained in abdominal SLNs, HSA800 was able to migrate to thoracic lymph nodes at time points greater than 1 hour.

Injection of Lymphatic Tracers into Different Quadrants of the Abdomen

Four groups of four rats each received either injection of QDs (Figure 3A) or HSA800 (Figure 3B) into each of the four quadrants of the abdomen. All rats were imaged 1 hour after injection of lymph tracers, as this permitted ample time for migration from the peritoneum into lymph nodes. The location and number of SLNs identified did not differ among the four groups. Nor was there a significant difference in the pattern of lymph flow based on the injection site.

Change of SLN Drainage Pattern after Bowel Resection

Six rats receiving bowel resection from the ligament of Treitz to the descending colon were compared to six control rats receiving laparotomy, bowel transection, and reanastomosis. All rats received intraperitoneal injection of QDs and imaging 1 hour later. After sham surgery, QD uptake was distributed to the superior mesenteric (6 out of 6 rats), celiac (4 out of 6 rats) and periportal (3 out of 6 rats) lymph node groups. This distribution was not significantly different from the distribution of QDs in non-operated rats. No sham surgery rats demonstrated intrathoracic QD uptake. After bowel resection, QD uptake was significantly shifted from intraabdominal lymph node groups to intrathoracic lymph node groups, namely the superior mediastinal (6 out of 6 rats) and anterior mediastinal (2 out of 6 rats) lymph node groups ($p<0.01$; Figure 4A). Only 3 of six bowel-resected rats had intraabdominal QD uptake. All three of these bowel-resected rats also had intrathoracic QD uptake. There was a significant change in the pattern of SLN drainage from abdominal lymph nodes to mediastinal lymph nodes following bowel resection.

Change in Distant Lymphatic Drainage Pattern after Bowel Resection

Six rats with bowel resection were compared to six sham controls. All received HSA800 and were imaged 1 hour later. Sham surgery rats had a distribution of HSA800 to the superior mesenteric (5 out of 6 rats), celiac (4 out of 6 rats), and periportal (6 out of 6 rats) lymph node groups, a distribution similar to non-operated rats. Three sham surgery rats did have uptake into the superior mediastinal lymph node group, and one had uptake into the anterior mediastinum lymph node group. In contrast, rats with maximal bowel resection had a significant increase in the number of intrathoracic lymph node groups with HSA800 uptake. All six bowel-resected rats had uptake into both the superior and anterior mediastinal lymph node groups ($p<0.01$, Figure 4B). Bowelresected rats also had a significant decrease in the

number of intraabdominal lymph nodes. While all 6 sham surgery rats had HSA800-positive intraabdominal lymph nodes, only 3 bowel-resected rats had intraabdominal HSA800 uptake. ($p<0.01$; Figure 4B). Additionally, in control rats, HSA800 could be seen within the thoracic duct and lymphatics within the diaphragm (Figure 5A). After bowel resection, HSA800 could not be seen within the thoracic duct but could be seen easily within parasternal and diaphragmatic lymphatics (Figure 5B), again demonstrating altered lymphatic drainage of the peritoneal cavity after bowel resection.

DISCUSSION

Flow of lymph from the peritoneum has been investigated in the context of peritonitis[11] and peritoneal dialysis.[12] Our study aims to investigate lymphatic drainage of the peritoneum in the context of the spread of cancer cells to regional lymph nodes and distant lymphatics. Stomach, colon, and ovarian cancer, and any malignancy with potential shedding of cells to the peritoneal space, may drain to a SLN with potential access to distant lymphatics. This study in the rat indicates that a specific peritoneal lymph drainage pattern exists. Although this pattern may vary among species, NIR fluorescent imaging is a means to identify peritoneal SLNs. Thus accurate nodal staging could be achieved without complete lymphadenectomy of several lymph node stations. Individual peritoneal SLNs could be identified and biopsied for staging, even before appreciable, bulky nodal disease or carcinomatosis occurs. For example, ovarian cancer with malignant cells in peritoneal washings can be staged as low as I_C depending on the primary tumor. However, involvement of distant lymph nodes is defined as stage III.[13] In routine staging laparotomy, the pelvic and para-aortic lymph nodes are sampled because of the lymph drainage pattern of the ovary. However, possible SLNs of the peritoneal space are not sought, identified, or purposely resected. Consequently, there is a potential for more accurate lymph node staging of cancers with potential shedding into peritoneal space.

Knowledge of lymph node drainage patterns could also aid in cytoreductive surgery in the setting of peritoneal carcinomatosis. Survival of patients with carcinomatosis from colorectal cancer, pseudomyxoma peritonei, and peritoneal mesothelioma increased based on the completeness of disease resection.[14–17] Similarly, with advanced uterine cancer, incomplete cytoreduction resulted in increased morbidity and mortality.[18] Therefore, identifying and assessing lymph nodes communicating with the peritoneal space can aid in completeness of resection and possibly survival.

In the rat model, there are specific NIR-fluorescent positive and negative nodes within each lymph node group, suggesting a particular lymph node drainage pattern, not merely diffusion into all intraabdominal lymphatics. In this study, we did not document the number of positive and negative lymph nodes within a group. However this would be a feasible study since NIR fluorescent imaging has the resolution to distinguish individual positive and negative nodes in both small and large animal models. [2,8,9,19–21] Since NIR fluorescent imaging is real-time, it should be possible to perform directed dissection of individual positive lymph nodes, which would obviate the need to do a complete lymphadenectomy of a lymph node station.

In the present study, we employed novel NIR fluorescent lymph tracers to identify the lymph drainage pattern of the peritoneum. The peritoneum can be considered as one lymph space with drainage to candidate lymph nodes, namely the celiac, periportal, and superior mesenteric lymph node groups. Abernethy et al. suggested that intrathoracic, not intraabdominal, lymph nodes were the primary recipient of lymph drainage of the peritoneal space.[6,22] They used Evans blue and ^{125}I-labeled human serum albumin as lymph tracers. These are smaller, more mobile molecules that may have passed through abdominal lymph nodes to concentrate in intrathoracic lymph nodes. In Abernathy et al.'s studies they did find some lightly blue-stained

intraabdominal lymph nodes, which may have been obscured by noted peritoneal surface staining.

We used differently-sized NIR lymph tracers that have several advantages over conventional lymph tracers. First, NIR fluorescent tracers fluoresce brightly through up to 1 cm of tissue.[8] The entire peritoneum and thorax can be imaged in real-time for *in situ* communicating nodes, thus maximizing sensitivity and minimizing sampling error. The images can also be magnified to assist in precise and complete resection of communicating lymph nodes. Second, NIR has insignificant background staining because *in vivo* tissue has minimal intrinsic NIR fluorescence. Third, and most important, the two differently-sized tracers allowed us to map the SLN with QDs and, in addition, map distant lymphatics beyond the SLN with HSA800.

In our study, the large 20-nm QDs did not pass through lymph nodes, but lodged and concentrated within the first node encountered, thus providing a more accurate identification of the SLN. Though some QD signal was found in superior mediastinal lymph nodes, these thoracic lymph nodes did not have the same convincing, bright presence as the intraabdominal lymph nodes. This suggests that the dominant drainage of the peritoneum is to intraabdominal SLN groups. It is possible that less important, but parallel, lymphatics drain the peritoneum directly to intrathoracic lymph nodes.

The optimal size of lymph tracers remains controversial, but it is thought to be in the range of 4–100 nm.[23,24] Cancer cells, which are much larger than lymph tracers, may also have the capacity to alter their own lymph flow. For example, tumor burden negatively affects the ability to identify SLNs in breast cancer because of altered lymph flow.[25] Therefore, study of smaller and distant lymph channels of the peritoneum was warranted. As QDs have been proven to be reliable and safe tracers for SLNs, HSA800 has proven to be a reliable tracer of lymphatic draining beyond the SLN. .[2,8,9,19–21]

At early time points, HSA800 identified the same candidate SLNs of the peritoneum as did QDs. Within 1 hour HSA800 identified communicating lymph channels with the thoracic duct, superior and anterior mediastinal lymph nodes and more faintly to the diaphragmatic and anterior chest wall lymphatics. Though the intraabdominal lymph node groups appear to be the SLNs of the peritoneal space, there is also communication, either in parallel or series, with diaphragmatic, thoracic duct, and chest wall lymphatics. Identification of intrathoracic lymph nodes and lymphatic channels corroborates findings of multiple studies with smaller lymph tracers.[4,26]

Given the large parietal and visceral surface area of the peritoneum, it is possible, therefore, that lymphatic drainage proceeds through multiple defined SLNs and lymphatics leading to the central circulation. These findings confirm previous studies of peritoneal space lymphatic drainage that also found multiple and parallel lymphatic drainage patterns.[22] Multiple SLNs are also found in SLN mapping of breast and melanoma.[27] In fact, the identification of multiple SLNs improved the false negative rate from 14.3% to 4.3% when only one SLN was identified.[28] The different permutations found from animal to animal of celiac, periportal, and superior mesenteric lymph node groups as SLNs indicate a complex and individualized lymphatic drainage pattern of the peritoneum. Drainage patterns could be specific to individual animals, species, or disease processes. These issues remain to be clarified; however, the development of NIR fluorescent lymph node mapping makes these future investigations feasible.

The candidate SLN groups, namely the celiac, periportal, and superior mesenteric lymph node groups are the same lymph node groups receiving lymph flow from the bowel. This suggests that the visceral, not the parietal side of the peritoneal space is the significant contributor of peritoneal lymphatic drainage. To further test this hypothesis, six rats received maximal bowel resection while still preserving continuity and periportal, celiac, and superior mesenteric lymph

node groups. Bowel-resected rats and sham surgery controls underwent intraperitoneal injection of QDs or HSA800 and imaging 1 hour later. After bowel resection, QDs identified peritoneal SLNs, to be intrathoracic, not intraabdominal. Furthermore, there was an absence of HSA800 in the thoracic duct and enhanced presence of HSA800 in diaphragmatic and anterior chest wall lymphatics. Therefore, lymphatics associated with the large and small intestine direct peritoneal lymph flow to intraabdominal SLNs, then to the thoracic duct, and finally to intrathoracic lymph nodes at later time points. In the absence of bowel lymphatics, the first draining lymph node group was actually intrathoracic, probably through diaphragmatic and anterior chest wall lymphatics (Figure 6). Therefore the visceral bowel surfaces, not the parietal surfaces of the peritoneum, govern peritoneal flow to select intraabdominal lymph nodes, followed by the thoracic duct and eventually to thoracic lymph nodes.

Of note, sham-surgery rats and non-operated rats did not always have QD or HSA800 uptake at the base of the mesentery. Possibly, the lymph of the peritoneum travels via subserosal lymphatics, spuriously intermixing with submucosal lymphatics of the bowel. It is possible that lymph could avoid contact with superior mesenteric lymph nodes altogether. The contribution of visceral surfaces to peritoneal space lymph drainage in humans is not fully appreciated. If our results in the rat are any indication, lymph flow to the bowel could be a novel mechanism of metastatic spread. Additionally, patients undergoing bowel resection could have an enhanced lymph flow from the peritoneal space through alternate lymph channels of the diaphragm and parietal surfaces.

In small and large animals, QDs and HSA800 have proven to be reliable and safe tracers for detection of SLNs.[2,8,9,19–21] A potential limitation of QDs and HSA800 is their unknown toxicity. With QDs, the individual metals comprising the inorganic core have known toxic effects, especially at concentrations higher than those used in our study. The toxicity of these metals when complexed as salts with an organic shell is unknown. In our studies, there were no signs of acute toxicity, namely changes in heart rate or rhythm, blood pressure, or oxygen saturation. HSA800 has greater potential for immediate clinical application since it is purely organic and the product of nontoxic components. However studies directed at establishing the toxicity, if any, of these tracers must still be performed before applying the technology to humans.

In conclusion, our findings of peritoneal SLN drainage to the celiac, periportal, and superior mesenteric lymph nodes of the rat cannot be extrapolated to humans. Indeed, our findings of redirected lymph drainage to the thorax in the presence of massive bowel resection compel further studies in large animal models and hopefully humans. In our rat model, we were able to appreciate intraabdominal lymph nodes with a laparotomy and intrathoracic lymph nodes with a thoracotomy. To make this technology more applicable to the clinical setting, we are actively developing the NIR fluorescent imaging system for a thoracoscope and laparoscope. Our findings do, however, indicate that the lymph drainage of the peritoneum is complex and individualized. NIR fluorescent imaging thus has potential to contribute to patient-specific, minimally invasive investigation of SLNs of the peritoneal space.

ACKNOWLEDGEMENTS

We thank Peter Kang, M.D. and Tomislav Mihaljevic, M.D. for helpful discussions, Barbara L. Clough for editing, and Grisel Rivera for administrative assistance. This work was supported in part by NIH NRSA # F32 HL72568-01 (C.P.P), the National Science Foundation - Materials Research Science and Engineering Center Program under grant DMR-0213282 (M.G.B.), NIH grants #R01-CA-115296 (J.V.F.) and R33-EB-000673 (J.V.F. and M.G.B.), and an Application Development Award (J.V.F.) from the Center for Integration of Medicine and Innovative Technology (CIMIT).

REFERENCES

1. Uren, RF.; Hoefnagel, CA. Lymphoscintigraphy. In: Thompson, JF.; Morton, DM.; Kroon, BBR., editors. Textbook of melanoma. London: Martin Dunitz; 2003. p. 339-364.
2. Parungo CP, Colson YL, Kim S, Kim S, Cohn LH, Bawendi MG, Frangioni JV. Sentinel Lymph Node Mapping of the Pleural Space. Chest. 2005In Press
3. Parungo CP, Ohnishi S, De Grand AM, et al. In vivo optical imaging of pleural space drainage to lymph nodes of prognostic significance. Ann Surg Oncol 2004;11:1085–1092. [PubMed: 15545502]
4. Fritz DL, Waag DM. Transdiaphragmatic lymphatic transport of intraperitoneally administered marker in hamsters. Lab Anim Sci 1999;49:522–529. [PubMed: 10551454]
5. Abu-Hijleh MF, Habbal OA, Moqattash ST. The role of the diaphragm in lymphatic absorption from the peritoneal cavity. J Anat 1995;186(Pt 3):453–467. [PubMed: 7559120]
6. Abernethy NJ, Chin W, Hay JB, Rodela H, Oreopoulos D, Johnston MG. Lymphatic drainage of the peritoneal cavity in sheep. Am J Physiol 1991;260:F353–F358. [PubMed: 2000952]
7. Cardenas A, Kelleher T, Chopra S. Review article: hepatic hydrothorax. Aliment Pharmacol Ther 2004;20:271–279. [PubMed: 15274663]
8. Kim S, Lim YT, Soltesz EG, et al. Near-infrared fluorescent type II quantum dots for sentinel lymph node mapping. Nat Biotechnol 2004;22:93–97. [PubMed: 14661026]
9. Ohnishi S, Lomnes SJ, Laurence RG, Gogbashian A, Mariani G, Frangioni JV. Organic alternatives to quantum dots for intraoperative near-infrared fluorescent sentinel lymph node mapping. Mol Imaging 2005;4:172–181. [PubMed: 16194449]
10. De Grand AM, Frangioni JV. An operational near-infrared fluorescence imaging system prototype for large animal surgery. Technol Cancer Res Treat 2003;2:553–562. [PubMed: 14640766]
11. Yuan Z, Rodela H, Hay JB, Oreopoulos D, Johnston MG. Lymph flow and lymphatic drainage of inflammatory cells from the peritoneal cavity in a casein-peritonitis model in sheep. Lymphology 1994;27:114–128. [PubMed: 7807984]
12. Tran L, Rodela H, Abernethy NJ, Yuan ZY, Hay JB, Oreopoulos D, Johnston MG. Lymphatic drainage of hypertonic solution from peritoneal cavity of anesthetized and conscious sheep. J Appl Physiol 1993;74:859–867. [PubMed: 8458807]
13. Greene, FL.; Balch, CM.; Page, DL.; Haller, DG.; Fleming, ID.; Morrow, M.; Fritz, AG. AJCC Cancer Staging Manual. Sixth ed.. New York: Springer-Verlag; 2002.
14. Begossi G, Gonzalez-Moreno S, Ortega-Perez G, Fon LJ, Sugarbaker PH. Cytoreduction and intraperitoneal chemotherapy for the management of peritoneal carcinomatosis, sarcomatosis and mesothelioma. Eur J Surg Oncol 2002;28:80–87. [PubMed: 11869020]
15. Verwaal VJ, van Ruth S, de Bree E, van Sloothen GW, van Tinteren H, Boot H, Zoetmulder FA. Randomized trial of cytoreduction and hyperthermic intraperitoneal chemotherapy versus systemic chemotherapy and palliative surgery in patients with peritoneal carcinomatosis of colorectal cancer. J Clin Oncol 2003;21:3737–3743. [PubMed: 14551293]
16. Verwaal VJ, van Tinteren H, van Ruth S, Zoetmulder FA. Predicting the survival of patients with peritoneal carcinomatosis of colorectal origin treated by aggressive cytoreduction and hyperthermic intraperitoneal chemotherapy. Br J Surg 2004;91:739–746. [PubMed: 15164445]
17. Witkamp AJ, de Bree E, Kaag MM, van Slooten GW, van Coevorden F, Zoetmulder FA. Extensive surgical cytoreduction and intraoperative hyperthermic intraperitoneal chemotherapy in patients with pseudomyxoma peritonei. Br J Surg 2001;88:458–463. [PubMed: 11260116]
18. Lambrou NC, Gomez-Marin O, Mirhashemi R, Beach H, Salom E, Almeida-Parra Z, Penalver M. Optimal surgical cytoreduction in patients with Stage III and Stage IV endometrial carcinoma: a study of morbidity and survival. Gynecol Oncol 2004;93:653–658. [PubMed: 15196860]
19. Parungo CP, Ohnishi S, Kim SW, et al. Intraoperative identification of esophageal sentinel lymph nodes using near-infrared fluorescence imaging. J. Thor. Cardiovasc. Surg. 2005In Press
20. Soltesz EG, Kim S, Laurence RG, et al. Intraoperative sentinel lymph node mapping of the lung using near-infrared fluorescent quantum dots. Ann Thorac Surg 2005;79:269–277. [PubMed: 15620956] discussion 269–77
21. Soltesz EG, Kim S, Kim SW, et al. Sentinel Lymph Node Mapping of the Gastrointestinal Tract by Using Invisible Light. Ann Surg Oncol. 2006In Press

22. Abernethy NJ, Chin W, Hay JB, Rodela H, Oreopoulos D, Johnston MG. Lymphatic removal of dialysate from the peritoneal cavity of anesthetized sheep. Kidney Int 1991;40:174–181. [PubMed: 1942765]

23. Noguchi M. Sentinel lymph node biopsy and breast cancer. Br J Surg 2002;89:21–34. [PubMed: 11851659]

24. Watanabe T, Kimijima I, Ohtake T, Tsuchiya A, Shishido F, Takenoshita S. Sentinel node biopsy with technetium-99m colloidal rhenium sulphide in patients with breast cancer. Br J Surg 2001;88:704–707. [PubMed: 11350445]

25. Wong SL, Edwards MJ, Chao C, Simpson D, McMasters KM. The effect of lymphatic tumor burden on sentinel lymph node biopsy results. Breast J 2002;8:192–198. [PubMed: 12100110]

26. Marco AJ, Domingo M, Ruberte J, Carretero A, Briones V, Dominguez L. Lymphatic drainage of Listeria monocytogenes and Indian ink inoculated in the peritoneal cavity of the mouse. Lab Anim 1992;26:200–205. [PubMed: 1501434]

27. McMasters KM, Reintgen DS, Ross MI, et al. Sentinel lymph node biopsy for melanoma: how many radioactive nodes should be removed? Ann Surg Oncol 2001;8:192–197. [PubMed: 11314933]

28. Wong SL, Edwards MJ, Chao C, et al. Sentinel lymph node biopsy for breast cancer: impact of the number of sentinel nodes removed on the false-negative rate. J Am Coll Surg 2001;192:684–689. [PubMed: 11400961]discussion 689–91

A.

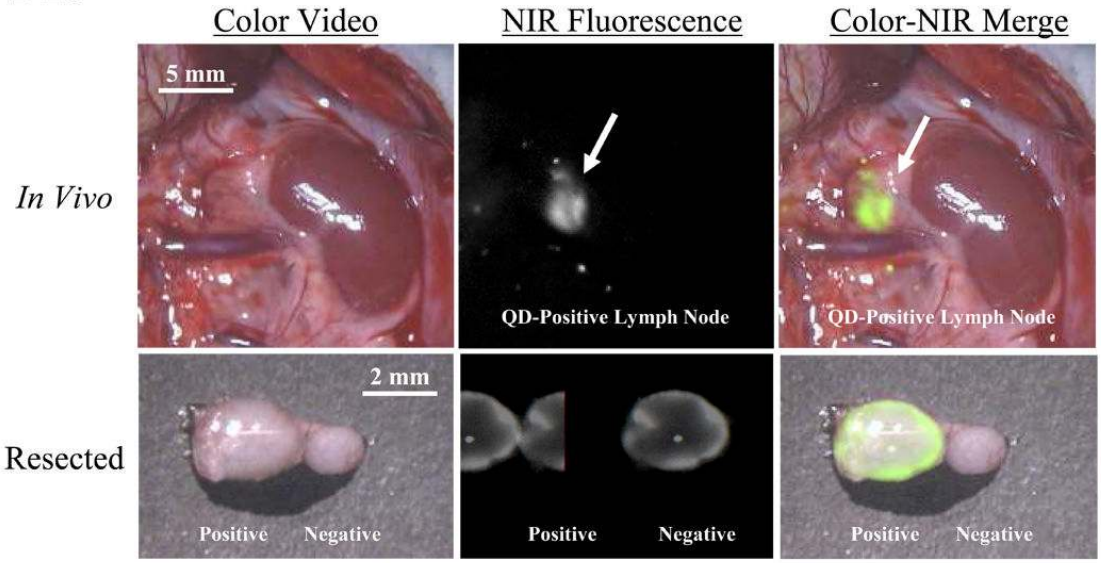

B.

Positive Lymph Nodes (x) after Peritoneal Injection of QDs

Time after Injection of QDs		Superior Mesenteric	Peri-portal	Celiac	Superior Mediastinal	Anterior Mediastinal
10 Minutes	Rat 1					
	Rat 2					
	Rat 3					
	Rat 4	x				
20 Minutes	Rat 5			x		
	Rat 6	x	x			
	Rat 7	x	x	x		
	Rat 8	x		x		
1 Hour	Rat 9	x				
	Rat 10	x	x	x		
	Rat 11	x	x	x		
	Rat 12	x		x		
4 Hours	Rat 13	x	x	x		
	Rat 14	x	x			
	Rat 15	x	x	x		
	Rat 16	x				
24 Hours	Rat 17	x	x	x		
	Rat 18	x	x			
	Rat 19	x		x		
	Rat 20	x		x		

Figure 1. Imaging and Quantification of Peritoneal Lymph Flow Using Large Hydrodynamic Diameter QDs

A) The top row shows an *in vivo, in situ* superior mesenteric lymph node with QD uptake (arrow). The bottom row shows this QD-positive lymph node and adjacent QD-negative lymph after resection. Shown are the color video (left column), NIR fluorescence (middle column), and merged images of the two (right column). B) Distribution of QDs injected into the peritoneal space and imaged at 10 minutes, 20 minutes, 1, 4, and 24 hours after injection. Uptake into intraabdominal lymph nodes can predictably be seen 20 minutes after injection, and up to 24 hours after injection.

A.

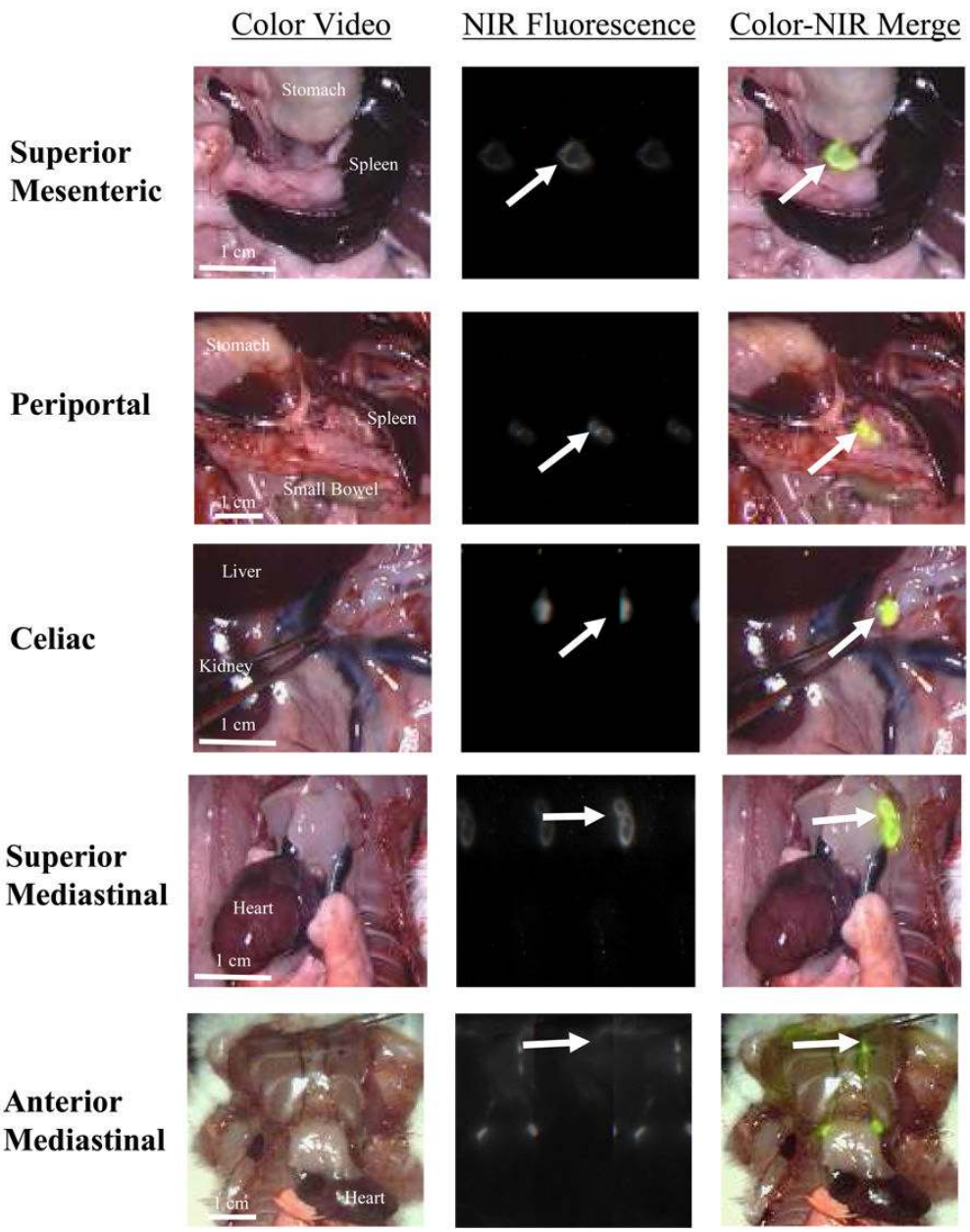

B.

Positive Lymph Nodes (x) after Peritoneal Injection of HSA800

Time after Injection of HSA-800		Superior Mesenteric	Peri-portal	Celiac	Superior Mediastinal	Anterior Mediastinal
10 Minutes	Rat 1					
	Rat 2	x				
	Rat 3					
	Rat 4	x				
20 Minutes	Rat 5	x	x	x		
	Rat 6	x	x	x		
	Rat 7	x	x	x	x	
	Rat 8	x	x			
1 Hour	Rat 9	x	x	x	x	
	Rat 10	x	x		x	
	Rat 11	x	x			
	Rat 12	x	x	x	x	x
4 Hours	Rat 13	x	x	x	x	
	Rat 14	x	x	x	x	
	Rat 15	x	x	x	x	
	Rat 16	x	x		x	x
24 Hours	Rat 17	x	x		x	
	Rat 18	x	x	x	x	x
	Rat 19	x	x	x	x	x
	Rat 20	x	x	x		

Figure 2. Imaging and Quantification of Peritoneal Lymph Flow Using Small Hydrodynamic Diameter HSA800

A) Examples of HSA800-positive lymph nodes (arrows) in each anatomic location. From top to bottom: Superior mesenteric, periportal, celiac, superior mediastinal and anterior mediastinal. Shown are the color video (left column), NIR fluorescence (middle column), and merged images of the two (right column). B) Distribution of HSA800 injected into the peritoneal space and imaged at 10 minutes, 20 minutes, 1, 4, and 24 hours later. Uptake into intraabdominal lymph nodes is seen reliably 20 minutes after injection and up to 24 hours after injection. Uptake of HSA800 into intrathoracic lymph nodes can be seen reliably 1 hour after injection and up to 24 hours after injection.

A.

Positive Lymph Nodes (x) after Peritoneal Injection of QDs into Each Abdominal Quadrant

Uptake 1 Hour after Injection of QDs		Superior Mesenteric	Peri-portal	Celiac	Superior Mediastinal	Anterior Mediastinal
Right Upper Quadrant	Rat 1	x		x		
	Rat 2	x		x		
	Rat 3	x	x			
	Rat 4	x				
Left Upper Quadrant	Rat 5	x		x		
	Rat 6	x	x			
	Rat 7	x	x	x		
	Rat 8	x	x			
Right Lower Quadrant	Rat 9	x		x		
	Rat 10	x	x			
	Rat 11	x	x			
	Rat 12		x	x		
Left Lower Quadrant	Rat 13		x	x		
	Rat 14	x		x		
	Rat 15	x		x		
	Rat 16	x		x		

B.

Positive Lymph Nodes (x) after Peritoneal Injection of HSA800 into Each Abdominal Quadrant

Uptake 1 Hour after Injection of HSA800		Superior Mesenteric	Peri-portal	Celiac	Superior Mediastinal	Anterior Mediastinal
Right Upper Quadrant	Rat 1	x	x	x	x	x
	Rat 2	x	x	x	x	x
	Rat 3		x	x	x	x
	Rat 4	x	x			
Left Upper Quadrant	Rat 5	x	x	x	x	x
	Rat 6	x	x	x	x	x
	Rat 7	x	x	x	x	x
	Rat 8	x		x		
Right Lower Quadrant	Rat 9	x	x	x		
	Rat 10	x	x			
	Rat 11	x		x	x	x
	Rat 12	x	x	x	x	x
Left Lower Quadrant	Rat 13		x	x	x	x
	Rat 14	x		x	x	x
	Rat 15	x	x	x		
	Rat 16	x	x	x	x	x

Figure 3. Location of Injection Does not Significantly Alter the Lymph Node Groups Identified

NIR fluorescent lymphatic tracers were injected into the right upper, left upper, right lower, or left lower quadrant and imaged 1 hour after injection A) There is no significant difference in the location of uptake of QDs, regardless of the intraperitoneal injection site. QDs, marking the sentinel lymph nodes, are seen within intraabdominal lymph nodes. B) There is no significant difference in the location of uptake of HSA800, regardless of injection site. HSA800, which identifies lymph flow beyond the sentinel lymph node, was seen within intraabdominal and intrathoracic lymph nodes one hour after injection into the peritoneal space.

A.

Positive Lymph Nodes (x) 1 Hour Post-Injection of QDs: Sham Surgery vs. Bowel Resection

Uptake 1 Hour after Injection of QDs		Superior Mesenteric	Peri-portal	Celiac	Superior Mediastinal	Anterior Mediastinal
Sham Surgery	Rat 1	x				
	Rat 2	x	x	x		
	Rat 3	x	x	x		
	Rat 4	x	x			
	Rat 5	x		x		
	Rat 6	x		x		
Bowel Resection	Rat 7				x	
	Rat 8				x	x
	Rat 9	x			x	
	Rat 10	x		x	x	
	Rat 11			x	x	
	Rat 12				x	x

B.

Positive Lymph Nodes (x) 1 Hour Post-Injection of HSA800: Sham Surgery vs. Bowel Resection

Uptake 1 Hour after Injection of HSA800		Superior Mesenteric	Peri-portal	Celiac	Superior Mediastinal	Anterior Mediastinal
Sham Surgery	Rat 1	x	x	x	x	
	Rat 2	x	x		x	
	Rat 3	x	x			
	Rat 4	x	x	x	x	
	Rat 5		x	x		
	Rat 6	x	x	x		
Bowel Resection	Rat 7	x			x	x
	Rat 8				x	x
	Rat 9				x	x
	Rat 10				x	x
	Rat 11			x	x	x
	Rat 12	x			x	x

Figure 4. Bowel Resection Alters Peritoneal Lymph Flow

A) Six rats receiving bowel resection, intraperitoneal QD injection, and imaging 1 hour later showed decreased QD uptake into intraabdominal lymph node groups and increased uptake into superior and anterior mediastinal lymph node groups compared to six sham surgery control rats. B) Six rats receiving bowel resection, HSA800 injection, and imaging 1 hour later showed increased uptake into superior and anterior mediastinal lymph node groups, elimination of uptake into periportal lymph node groups, and decreased celiac and superior mesenteric lymph node uptake compared to six control rats.

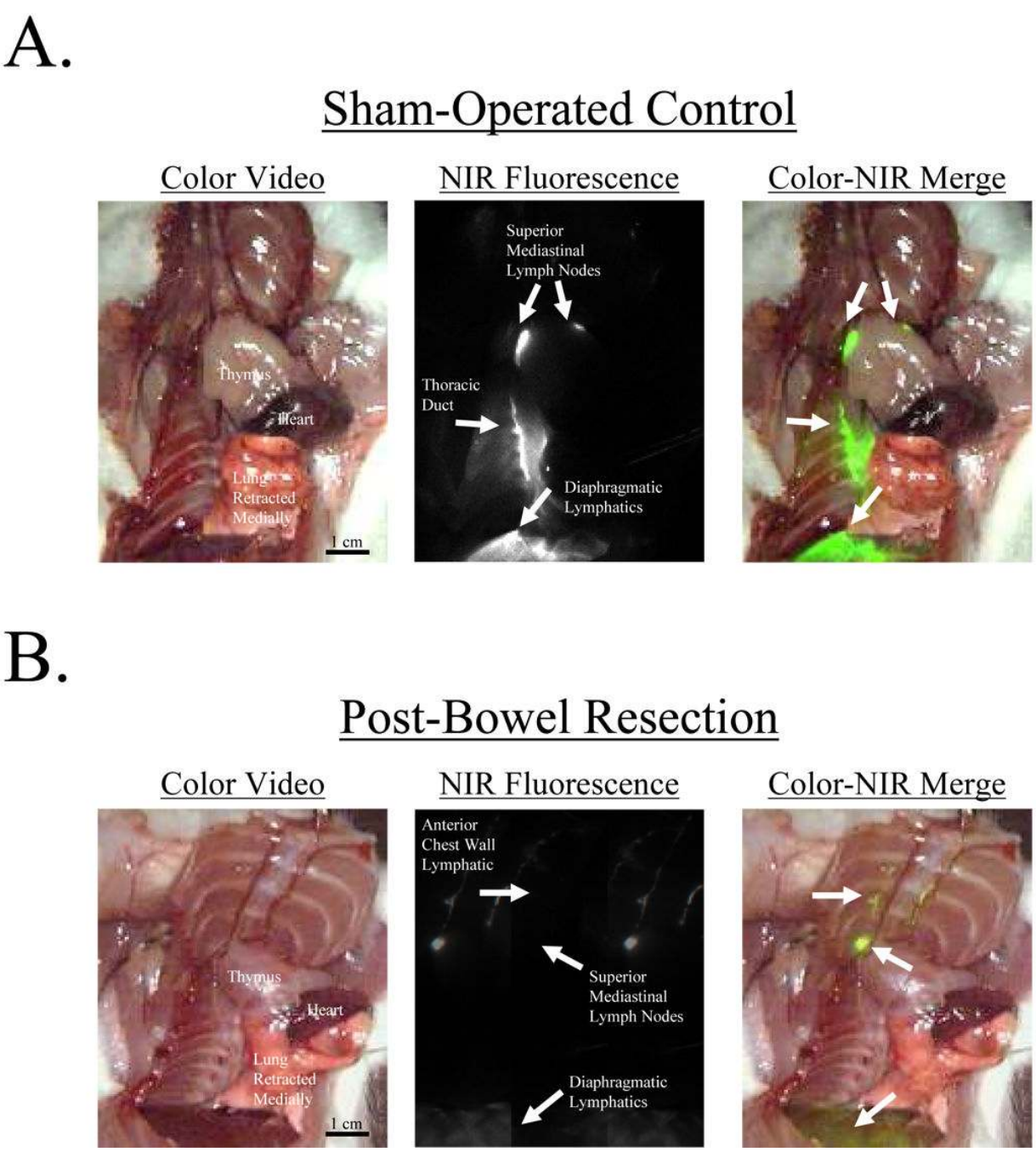

Figure 5. HSA800 Distribution Pre- and Post-Bowel Resection

A) HSA800 injected into the peritoneal space and imaged 1 hour later shows uptake into lymphatics of the diaphragm, the thoracic duct, and superior mediastinal lymph nodes in a sham control rat. B) After bowel resection from the ligament of Treitz to the descending colon and anastomosis, HSA800 was injected into the peritoneal space and imaged 1 hour later. HSA800 flow through the thoracic duct is eliminated, but enhanced parasternal lymphatic flow and superior mediastinal lymph node uptake is seen. Shown are the color video (left column), NIR fluorescence (middle column), and merged images of the two (right).

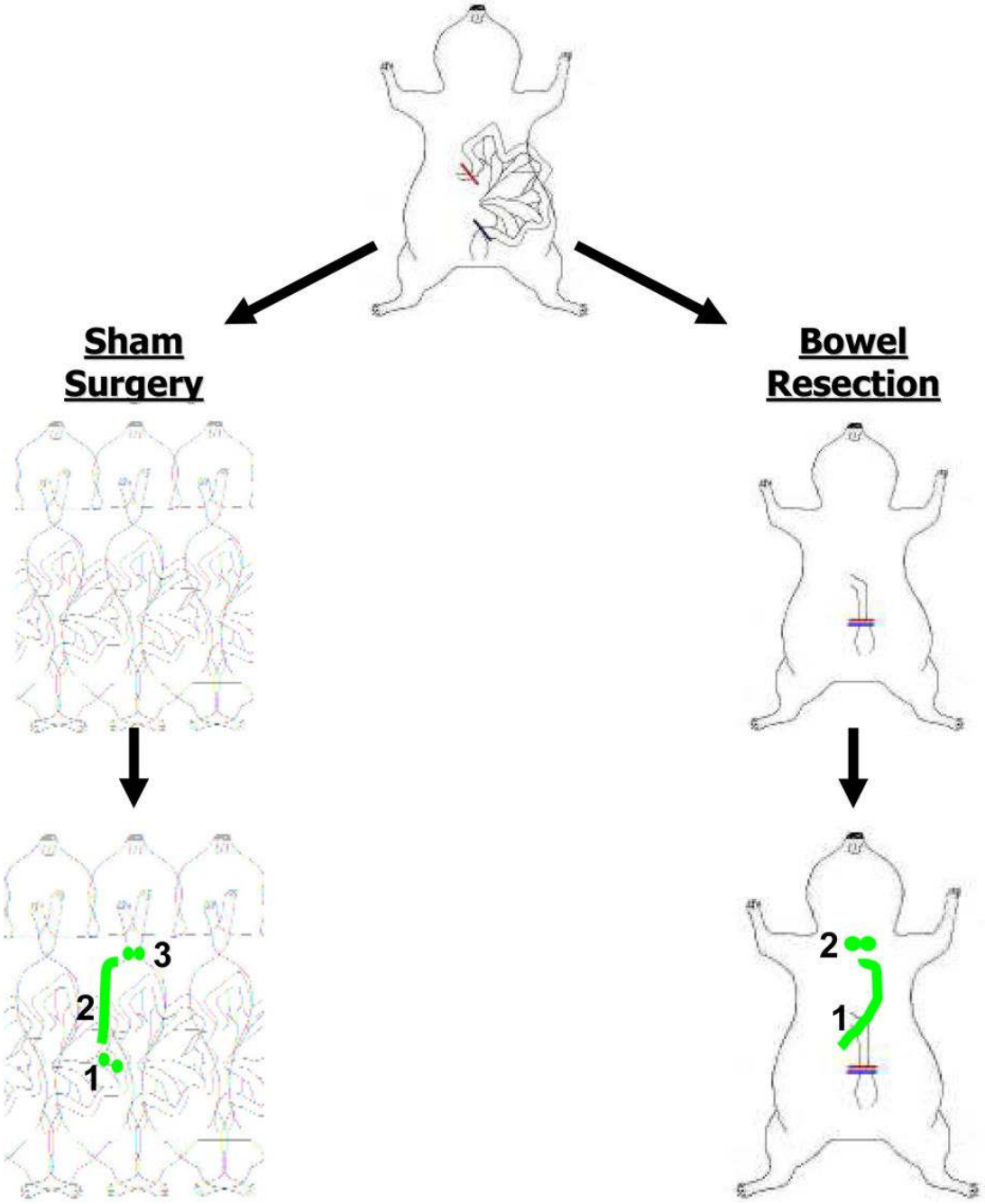

Figure 6. Flow of Lymph from the Peritoneal Space and Changes in Flow Post-Bowel Resection

Peritoneal lymph is directed to: 1) Intraabdominal SLN groups (superior mesenteric, periportal and celiac), 2) the thoracic duct, and 3) eventually mediastinal lymph nodes. Post-bowel resection, peritoneal lymph is directed to: 1) anterior chest wall lymphatics and 2) intrathoracic SLNs.